Journal of Materials Chemistry C

REVIEW

View Article Online
View Journal | View Issue

Cite this: J. Mater. Chem. C, 2016, 4, 5890

An overview of multifunctional epoxy nanocomposites

Hongbo Gu,*[a] Chao Ma,[a] Junwei Gu,†*[b] Jiang Guo,[c] Xingru Yan,[c] Jiangnan Huang,[c] Qiuyu Zhang[b] and Zhanhu Guo*[c]

Received 23rd March 2016,
Accepted 12th May 2016

DOI: 10.1039/c6tc01210h

www.rsc.org/MaterialsC

Epoxy is a crucial engineered thermosetting polymer with wide industrial applications in adhesive, electronics, aerospace and marine systems. In this review, basic knowledge of epoxy resins and the challenge for the preparation of epoxy nanocomposites are summarized. The state-of-art multifunctional epoxy nanocomposites with magnetic, electrically conductive, thermally conductive, and flame retardant properties of the past few years are critically reviewed with detailed examples. The applications of epoxy nanocomposites in aerospace, automotives, anti-corrosive coatings, and high voltage fields are briefly summarized. This knowledge will have great impact on the field and will facilitate researchers in seeking new functions and applications of epoxy resins in the future.

1. Introduction

Epoxy, as one of the most widely used conventional thermosetting plastics, has wide industrial applications including adhesives,[1–4] electronic devices (as excellent electrical insulators),[5] laminates,[6] encapsulations (covering the integrated circuitry from harsh environments[7]),[8] coatings,[9–11] marine systems,[12–14] and aerospace parts[15–18] owing to its high tensile strength and Young's modulus, thermal stability, solvent resistance, and good thermal insulation.[19–21] Liquid epoxy resins, a class of highly reactive prepolymers with low molecular weight oligomers that contain oxirane structures as an "epoxy" functionality (Fig. 1(a)), can contain either aliphatic, aromatic, and/or heterocyclic structures in the backbone.[22] Different backbone structures endow epoxy resins with different physical properties. For example, a short chain aliphatic epoxy resin (*e.g.* diglycidyl ether of hexanediol) has a low viscosity, while an aromatic epoxy resin (*e.g.* diglycidyl ether of bisphenol F or A) exhibits better thermal performance

[a] Shanghai Key Lab of Chemical Assessment and Sustainability, Department of Chemistry, Tongji University, Shanghai, 200092, China. E-mail: hongbogu2014@tongji.edu.cn
[b] Department of Applied Chemistry, School of Science, Northwestern Polytechnical University, Xi'an, Shaanxi, 710072, China. E-mail: gjw@nwpu.edu.cn
[c] Integrated Composites Lab (ICL), Department of Chemical & Biomolecular Engineering, University of Tennessee, Knoxville, Tennessee, 37966, USA. E-mail: zguo10@utk.edu
† The author Junwei Gu contributed equally to this work and should be considered as a co-first author.

Hongbo Gu

Dr Hongbo Gu, received her PhD degree at the Harbin Institute of Technology (HIT) in Jan. 2014, China. During her graduate study, she worked as a joint Chemical Engineering PhD student with Prof. Zhanhu Guo at Lamar University sponsored by the China Scholarship Council (CSC). Currently, she is an Assistant Professor at Tongji University (TJU) in China. Her research interests focus on giant magneto-resistance (GMR) sensors, multi-functional polymer nanocomposites especially magnetic and conductive materials for environmental remediation and electronic devices.

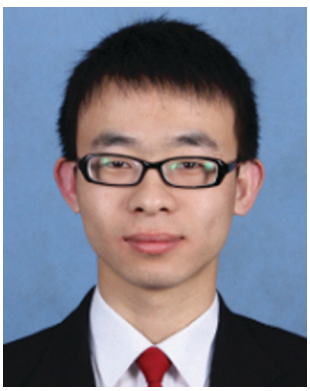

Chao Ma

Chao Ma, received his Bachelor's degree at Tongji University (TJU) in July 2012, China. After his undergraduate study, he worked as a research and development engineer of modified plastics at the Heilongjiang Xinda Enterprise Group Co., Ltd from Mar. 2013 to Aug. 2015, China. Currently, he is a master student at TJU. His research interests focus on the preparation and applications of multifunctional epoxy nanocomposites.

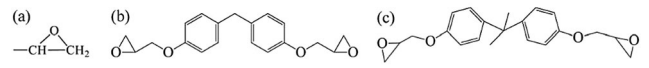

Fig. 1 Chemical structure of (a) oxirane structure as an "epoxy" functionality, (b) bisphenol F (Epon 862), and (c) bisphenol A (D.E.R. 331) resin.

such as a high glass transition temperature (T_g).[23] Examples of aromatic epoxy resins are diglycidyl ether of bisphenol F (DGEBPF) and diglycidyl ether of bisphenol A (DGEBPA). DGEBPF, such as Epon 862 resin, is an epoxidized novolac resin with high molecular weight variations. DGEBPA, such as D.E.R. 331 resin, is the largest productive epoxy resin for industrial sites.[23] Their explanatory chemical structures are shown in Fig. 1(b) and (c). Epoxy resin superiority to polyester, phenolic and melamine resins lies in its no volatile loss and little shrinkage during the curing process, good chemical resistance and inertness as well as versatility in selecting curing agents and conditions.[24] The tough, insoluble, and infusible epoxy is normally formed *via* a cross-linking reaction (also called the curing process or solidification) of liquid epoxy resins with hardeners (also called catalysts or curing agents) including polyfunctional amines, acids (or acid anhydrides), phenols, alcohols, and thiols.[25] The types of resins and curing agents are reported to influence the properties of the final epoxy finish. Generally, higher tensile strengths, glass transition temperatures and stiffness are obtained in the high-temperature cured epoxy system compared to those in the low-temperature cured epoxy system.[26] Fig. 2 and 3 show the curing process of anhydride–D.E.R 331 resin and amine–Epon 862 resin systems, respectively.

Recently, epoxy nanocomposites have gained great interest due to their unique physicochemical properties arising from the combined special characteristics of the nanoparticles and epoxy into one unity.[28] Novel multifunctional epoxy nanocomposites are defined as the combination of better structural performances with smart features such as strain monitoring, sensing, and actuation capabilities.[29] In order to improve the mechanical properties and to introduce new functionalities such as electrical conductivity, magnetic and optical properties, various nanostructural materials including carbon nanofibers (CNFs),[2] carbon nanotubes (CNTs),[30,31] iron and iron oxide nanoparticles,[32] graphene,[33,34] nanoclay,[35,36] polyaniline (PANI),[37] silica,[38,39] zinc oxide[40–42] and alumina[43] have been used to prepare epoxy nanocomposites. This can provide epoxy with unique properties such as optical,[44] anticorrosive,[45] electrical[46,47] and magnetic properties.[48] Though there are several comprehensive reviews on the thermal decomposition, combustion, and flame-retardancy of epoxy systems,[22] and on epoxy nanocomposites with surface-modified silicon dioxide nanoparticles,[23] a review on multi-functional epoxy nanocomposites is still rare so far. In this review, the challenges and possible solutions for preparing epoxy nanocomposites are presented. The multifunctional epoxy nanocomposites and their applications of the past few years are critically reviewed with detailed examples in order to provide basic knowledge to meet the demands of current epoxy nanocomposites in industrial applications.

2. Challenges and solutions for the preparation of epoxy nanocomposites

Generally, owing to the higher ratio of surface to volume, nanoparticles much prefer to be arranged adjacently and attract each other to form agglomerations. Therefore, during the preparation process of multifunctional epoxy nanocomposites, two main challenges remain in obtaining the strengthened epoxy nanocomposites, *i.e.*, nanofiller dispersion and interfacial nanofiller–polymer interaction.[49–51] The polymer–nanofiller interfaces can serve as crack initiating points to deteriorate the mechanical

Junwei Gu

Dr Junwei Gu, currently an Associate Professor of Materials Science at Northwestern Polytechnical University, obtained a Materials Science PhD degree from Northwestern Polytechnical University (2010). His current research focuses on structure designing, performance control and mechanisms of thermally conductive polymeric composites, designing, preparation and processing of structure/function integrating for fibers/polymer matrix composite materials, and surface/interface modification, mechanisms and numerical simulation of organic/inorganic hybrid materials.

Zhanhu Guo

Dr Zhanhu Guo, currently an Associate Professor of Chemical Engineering at the University of Tennessee, obtained a Chemical Engineering PhD degree from Louisiana State University (2005) and received three-year (2005–2008) postdoctoral training in the Mechanical and Aerospace Engineering Department at the University of California Los Angeles. Dr Guo, the Chair of the Composite Division of the American Institute of Chemical Engineers (AIChE, 2010–2011), directs the Integrated Composites Laboratory (ICL) with more than 20 members. His current research focuses on fundamental science behind multifunctional nanocomposites for energy harvesting, electronic devices, environmental remediation, anti-corrosion, fire-retardancy, and electromagnetic radiation shielding/absorption applications.

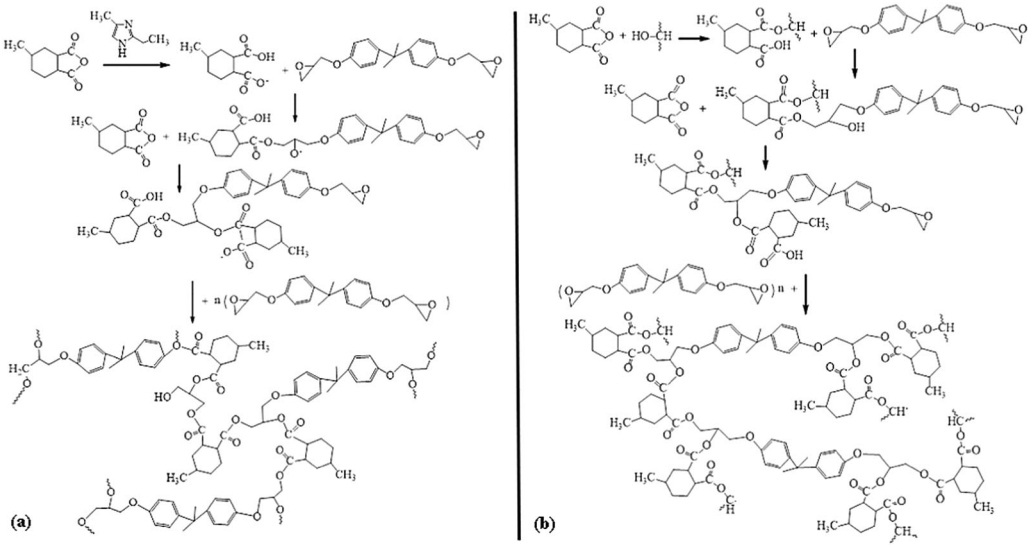

Fig. 2 Curing process of anhydride–D.E.R. 331 system (a) with accelerator, and (b) without accelerator.[27]

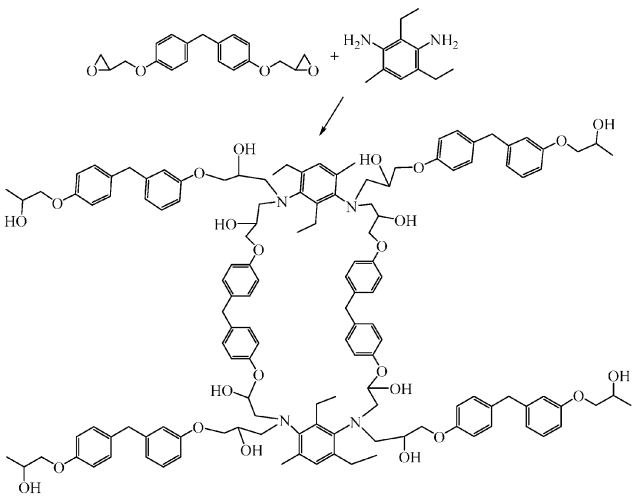

Fig. 3 Curing process of amine–Epon 862 system.

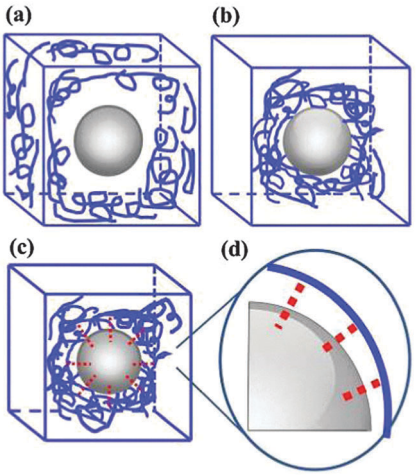

Fig. 4 (a) Voids between nanofiller and matrix; (b) polymer wrapping; (c) covalent bonding; and (d) an enlarged illustration of (c) to show the increased chemical bonding density.

properties of the polymer. Normally, a fine nanoparticle dispersion can be obtained by surface treatment with proper surfactants, polymers or coupling agents[50,52–54] and effective stirring. Different physical stirring methods have been explored to disperse nanofillers including mechanical stirring, shear mixing, magnetic stirring, three roller milling, bead milling, ultrasonic horn stirring, and ultrasonic bath stirring.[55] The results showed that the stirring methods had a significant effect on the dispersion quality, and even on the microstructures and properties of the formed products. For example, iron oxide nanoparticles were etched completely if mechanical stirring was used for conductive polypyrrole (PPy) formation. However, ultrasonication resulted in core–shell iron oxide–PPy structural composites.[56]

Meanwhile, voids which exist between the nanofillers and the hosting polymer matrix, Fig. 4(a), will reduce the mechanical properties of the polymer. Two methods can be used to solve this interaction challenge. One is the weak physical wrapping of polymer chains on the nanofillers *via* van der Waals forces, hydrogen bonding, electrostatic, steric, and Lewis acid–base interactions. The physically adsorbed polymer chains or surfactants can minimize voids to enhance the mechanical properties, Fig. 4(b). The other is to introduce strong chemical covalent bonding between the nanofillers and the hosting polymer matrix with the aid of a coupling agent, polymer or surfactant, Fig. 4(c). The bonding density of bridging can be increased by grafting denser coupling agents to improve the mechanical properties further, Fig. 4(d). The first method is usually used for preparing inert polyolefin nanocomposites like polypropylene (PP) reinforced with CNTs.[57,58] For example, PP grafted maleic-anhydride (PP-*g*-MA) has been used as a coupling agent by He *et al.*[59] to modify the CNT surface aiming to increase the compatibility between PP and the CNTs by minimizing voids.

In the second method, surface modification is a common way to improve the nanofiller dispersion level and to enhance the interfacial polymer–nanofiller interactions[46] through proper coupling agents,[2,50,60,61] surfactants[62] and polymers,[17,18,21,61,63–67] in which the surface modifiers should be compatible with the hosting polymers. In this case, the surface modification can be categorized as two types: covalent and noncovalent functionalization.[68] Lee *et al.*[69] put noncovalently functionalized hexagonal boron nitride nanoflakes (BNNF) with 1-pyrenebutyric acid (PBA) into epoxy resin, which was able to attach the target functional groups on the surface of the nanofiller without any loss of nanofiller properties. In the BNNF/epoxy nanocomposites with a BNNF loading of 0.3 wt%, an elastic modulus of up to 3.34 GPa was obtained and the ultimate tensile strength was up to 71.9 MPa, which were increased by about 21% and 54% compared with the pure epoxy, respectively.[69] This high performance resulted from the strong affinity between the nanofiller and the epoxy matrix and the homogeneous dispersion of nanofiller within the epoxy matrix due to the noncovalent functionalization. In the following text, the covalent functionalization method using coupling agents is discussed.

2.1 Silane coupling agents

Commonly used coupling agents are silanes, which contain at least two different functional groups, Fig. 5(a). One functional group can form chemical bonds with the nanofiller, and the other can attach to the hosting matrix, Fig. 5(b). Coupling agents are normally used to provide a stable bonding bridge between the nanofiller and the hosting matrix,[70] which can transfer the applied load from the weak polymer to the stronger nanofiller to yield an enhanced reinforcement performance and provide the polymer matrix with a longer service life.[21,71] 3-Aminopropyltriethoxysilane (APTES), as one type of silane, has been used to functionalize the surface of CNFs *via* salinization to favor CNF dispersion and improve the interfacial interaction between the CNFs and the epoxy monomer *via* the formed chemical bonding, Fig. 5(c). The alkoxy groups from APTES were found to be attached to the carboxyl groups on the surface of the CNFs, and the amine groups on APTES was reacted with the epoxide groups of the epoxy monomer. However, the required refluxing in the salinization process might damage the properties of the nanofiller.[2] Another kind of silane, 3-glycidoxypropyltrimethoxysilane (GPTMS), was used as the coupling agent to improve the dispersion quality of multi-walled carbon nanotubes (MWNTs)

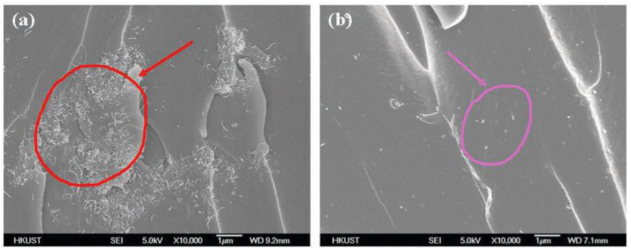

Fig. 6 SEM images of fracture surfaces for epoxy nanocomposites showing the dispersion properties of MWNTs: (a) 0.25 wt% as-received MWNTs; and (b) 0.25 wt% silane–MWNTs. Reprinted with permission from Elsevier.[72]

within an epoxy matrix.[72] The fracture surfaces of cured epoxy nanocomposites are depicted in Fig. 6 in order to provide insight into the dispersion properties of MWNTs in epoxy. The as-received MWNTs are observed to be severely agglomerated in the epoxy matrix (red colored part with arrow), whereas the silane treated MWNTs are more uniformly dispersed within the epoxy matrix (purple colored part with arrow), illustrating a better nanofiller dispersion quality after the introduction of silanes on the surface of the nanofiller. The better MWNT dispersion and increased interfacial interaction due to the salinization reduced the mobility of the epoxy matrix around the MWNTs and improved the thermal stability and storage modulus at elevated temperatures.

2.2 Conducting polymer coupling agents

Recently, conducting polymers including PANI[18,21,66,73] and PPy,[17] which were introduced onto the surface of nanofillers by a surface initiated polymerization (SIP) method, have been reported to serve as coupling agents to improve the nanoparticle dispersion and enhance the interfacial interactions between the nanoparticles and the epoxy. For example, Fig. 7 depicts the cross-sectional surface of cured as-received, and PANI functionalized Fe_3O_4/epoxy nanocomposites. The as-received Fe_3O_4 nanoparticles were observed to be agglomerated to form bigger particles due to few functional groups on the surface of the nanoparticles and the intraparticle magnetic dipole–dipole interactions, Fig. 7(a).[74] However, the PANI functionalized Fe_3O_4 nanoparticles were observed to be uniformly dispersed within the epoxy matrix in the cross-sectional surface image of the cured epoxy nanocomposite, Fig. 7(b),[73] confirming the coupling role of PANI.

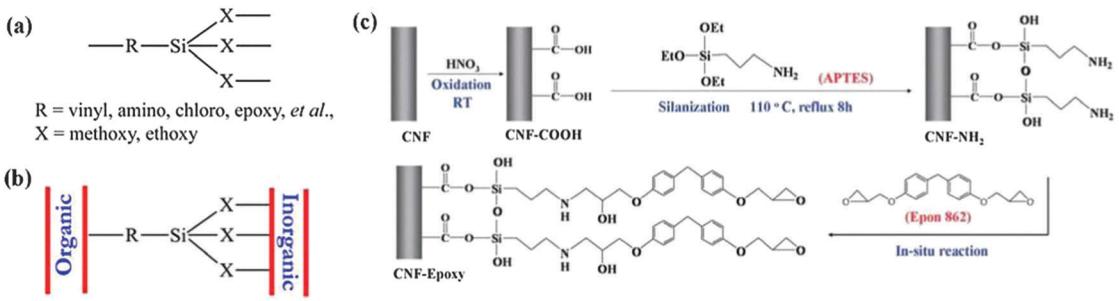

Fig. 5 (a) Chemical structures of coupling agent silanes, and (b) the bridging effect between the matrix and the inorganic fillers; (c) salinization process of the CNFs and curing mechanism of the APTES functionalized CNFs with the epoxy monomer.[2]

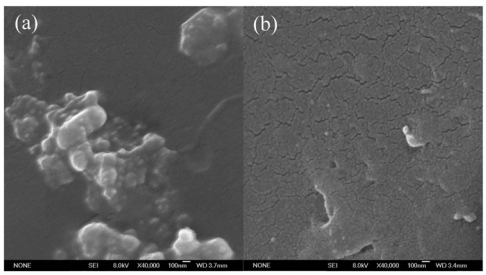

Fig. 7 Particle distribution on the cross-sectional surface of cured epoxy nanocomposites filled with 5 wt% loading of (a) as-received Fe_3O_4 and (b) PANI functionalized-Fe_3O_4 nanoparticles after polishing.[73]

After functionalization with PANI, the tensile strength of the epoxy was observed to be increased by 15.7%, 85.0%, and 28.4% in the epoxy filled with 5.0 wt% Fe_3O_4 nanoparticles,[73] 0.7 wt% MWNTs,[21] and 1.0 wt% silica nanoparticles, respectively, due to the improved nanofiller distribution.[18] Especially, the T_g, which is used to describe the crosslinking degree of materials, was improved by about 25 °C in the epoxy system filled with 0.7 wt% MWNTs.[21] The possible chemical reaction between the PANI functionalized nanofiller and the epoxy monomer was monitored by DSC measurements, Fig. 8. For the epoxy monomers (Fig. 8A(b) and B(b)) and the epoxy monomer suspension with the as-received nanofiller (Fig. 8B(a)), there was no exothermic peak observed during the whole procedure. However, a curing exothermic peak at around 110 °C and an endothermic peak at around 90–100 °C were obviously observed in the epoxy suspension with the PANI functionalized Fe_3O_4 nanoparticles (Fig. 8A(a)) and with the PANI functionalized MWNTs (Fig. 8B(c)), respectively. These peaks illustrated that PANI had reacted with the epoxy resin monomers due to the presence of amine groups. The proposed curing processes of the epoxy nanocomposites in the presence of PANI and PPy are shown in Fig. 9 and 10, respectively.

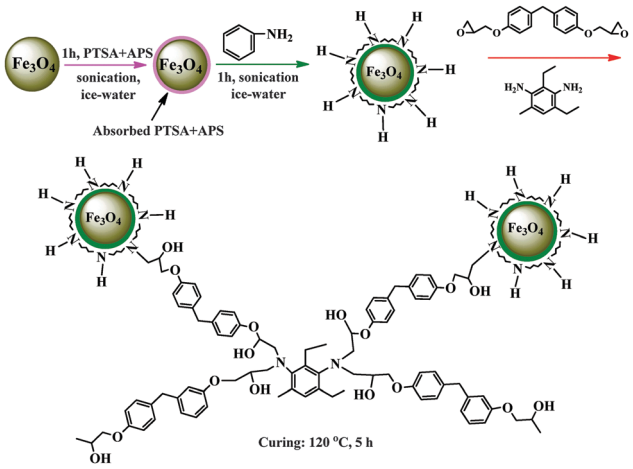

Fig. 9 Curing process of PANI functionalized Fe_3O_4/epoxy nanocomposites.[73]

3. Applications of multifunctional epoxy nanocomposites

3.1 Epoxy nanocomposites with magnetic properties

Normally, magnetic epoxy nanocomposites can be achieved through the introduction of magnetic nanoparticles into the epoxy matrix. This can broaden the engineered applications of epoxy in the fields of microwave adsorption,[75–77] magnetic resonance imaging (MRI),[53] electromagnetic interference (EMI) shielding, and flexible electronics.[73] Recently, magnetic nanoparticles, such as iron, cobalt, nickel and their alloys among them or with others, have received considerable attention in different chemistry and physics fields[78] due to their unique physicochemical properties including high coercivity (H_c, Oe) and inherent active chemical catalysis with their small size and high specific surface area, which are different from the bulk materials.[79] Generally, in magnetic hysteresis loops, H_c stands for the intensity of the applied external magnetic field that is required to return the material to zero magnetization conditions after the materials have reached saturation, and the remnant magnetization (M_r) is the residue magnetization after the applied external magnetic field is removed. Bulk magnetic materials consist of different magnetic domains, in which the magnetic moments of atoms are aligned in the same direction. However, as the size of a magnetic material is reduced, the number of magnetic domains will be decreased, even to one single domain. In this case, the magnetic properties of these nanoparticles are no longer consistent with the bulk magnetic materials.[80] Owing to their small size on the nanoscale, the magnetic nanoparticles exhibit more efficient interactions with the polymer matrix,

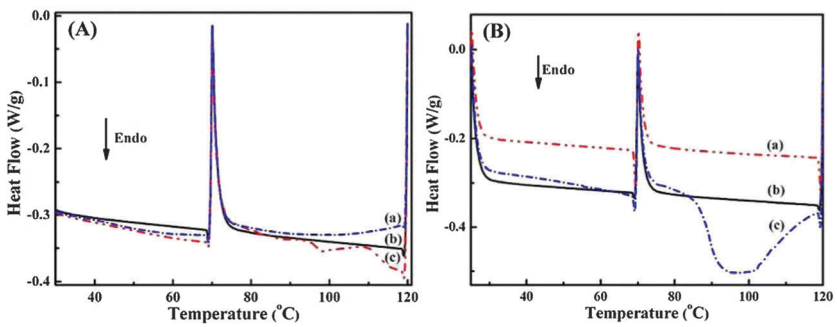

Fig. 8 DSC curves of (A) (a) epon suspension with f-Fe_3O_4 nanoparticles, (b) epon monomers, (c) epon suspension with PANI nanoparticles;[73] (B) (a) epoxy monomer suspension with u-MWNTs, (b) epoxy monomer, (c) epoxy suspension with f-MWNTs.[21]

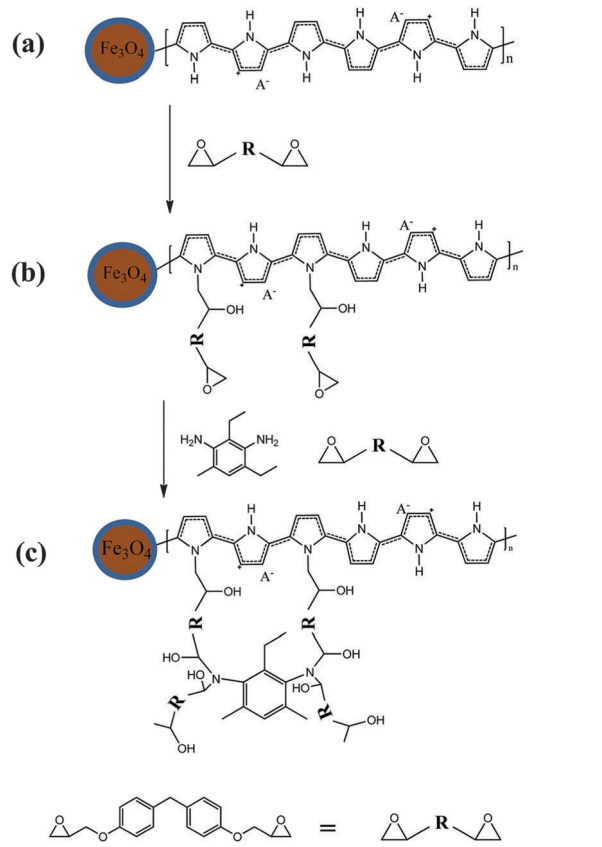

Fig. 10 Curing process of PPy functionalized Fe_3O_4/epoxy nanocomposites.[17]

which influence the surface energy at the interface between the magnetic nanoparticles and the matrix.[81] Among all the magnetic nanoparticles, magnetite (Fe_3O_4) is the strongest magnetic material of all natural minerals on Earth.[82] Park *et al.*[83] prepared the silane modified Fe_3O_4/epoxy nanocomposites and studied their magnetic properties and wear rates. The saturation magnetization of the modified Fe_3O_4/epoxy nanocomposites was observed to be larger than that of the unmodified Fe_3O_4/epoxy nanocomposites. The specific wear rate of the surface modified Fe_3O_4/epoxy nanocomposites was lower than that of the unmodified Fe_3O_4/epoxy nanocomposites due to the increased nanoparticle dispersion quality within the epoxy matrix. Gu *et al.*[73] prepared magnetic PANI functionalized Fe_3O_4/epoxy nanocomposites, which showed good magnetic properties and could be attracted by a permanent magnet, Fig. 11(A). In Fig. 11(A), the as-received Fe_3O_4 nanoparticles, PANI functionalized Fe_3O_4 nanoparticles, and PANI modified Fe_3O_4/epoxy nanocomposites show no magnetic hysteresis loops, indicating superparamagnetic behavior.[84] Guo *et al.*[17] fabricated magnetic PPy functionalized Fe_3O_4/epoxy nanocomposites. The calculated magnetic moment based on the Langevin equation was observed to be similar for the Fe_3O_4 nanoparticles, the PPy functionalized Fe_3O_4 nanoparticles and the Fe_3O_4/epoxy nanocomposites, indicating that the PPy and the epoxy matrix had little effect on the magnetic moment of the Fe_3O_4 nanoparticles.

However, owing to the easy oxidation and the flammability of pure magnetic metal nanoparticles in air, most reported magnetic nanocomposites have been prepared based on the magnetic metal oxide (such as Fe_3O_4).[85] More often, a protective layer including carbon or oxide was introduced to the surface of pure metal to solve the oxidation challenges for pure magnetic metal nanoparticles. For example, the prepared Fe@FeO,[32] Fe@Fe_2O_3,[86] and Fe@C[81] nanoparticles were mixed with epoxy to form the magnetic epoxy nanocomposites. In the Fe@FeO/epoxy nanocomposites, the tensile strength was well maintained even at high nanoparticle loadings of up to 20 wt%. The H_c value for the Fe@FeO nanoparticles was increased from 62.33 to 202.13 Oe after the nanoparticles were dispersed into the epoxy matrix (as shown in Fig. 11(B)), arising from the enlarged nanoparticle space distance among the nanoparticles, which led to a decreased interparticle dipolar interaction.[32] In the Fe@Fe_2O_3/epoxy nanocomposites, graphene nanosheets were used as a second nanofiller for the epoxy matrix. In these epoxy nanocomposites, the tensile strength when filled with 1.0 wt% graphene/Fe@Fe_2O_3 was 58% higher than that of the pure epoxy. The H_c value was seen to decrease with increasing graphene/Fe@Fe_2O_3 nanoparticle loadings.[86] In the Fe@C/epoxy nanocomposites, the tensile strength with 5.0 wt% loading of Fe@C nanoparticles was 60% higher than that of the pure epoxy. The H_c value of the Fe@C nanoparticles exhibited a similar trend to that of the Fe@FeO nanoparticles in the Fe@FeO/epoxy nanocomposites and increased after

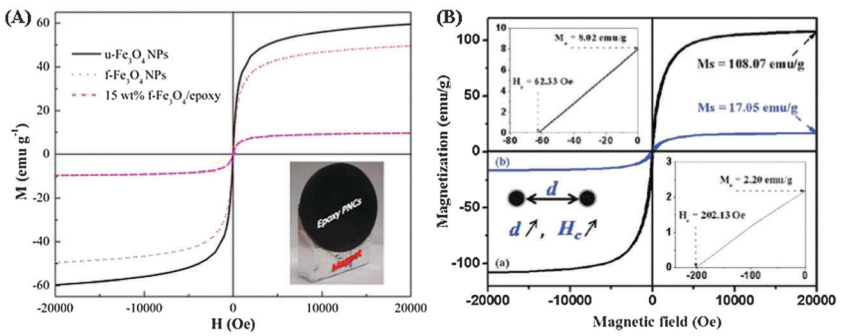

Fig. 11 Room-temperature hysteresis loops of (A) as-received Fe_3O_4 (u-Fe_3O_4), PANI functionalized Fe_3O_4 nanoparticles (f-Fe_3O_4) and an epoxy nanocomposite filled with 15 wt% f-Fe_3O_4 nanoparticles. Inset shows that the prepared epoxy nanocomposites could be attracted by a permanent magnet;[73] (B) (a) Fe@FeO nanoparticles and (b) 20 wt% Fe@FeO/epoxy nanocomposite.[32]

adding the Fe@C nanoparticles into the epoxy matrix as compared to the pure Fe@C nanoparticles.

3.2 Epoxy nanocomposites with electrical and thermal conductivities

The rapid development of the semiconductor electronic industry, especially wireless telecommunication, demands new multifunctional nanocomposites to achieve the requirements of electronic devices.[87] Therefore, epoxy based nanocomposites with electrical and thermal conductivities have emerged due to their environmentally friendly and cost effective process/materials, and potential for large-scale production.[88] Normally, nanoparticles are superior to micron sized particles in electrically and thermally conductive applications since the higher specific surface area of nanoparticles can enhance the electrical and thermal properties, giving, for example, a reduced percolation threshold and improved electrical and thermal conductivity.[89] Thus, on one hand, while different conductive nanofillers[90] including graphene, CNTs, CNFs, conducting polymers PANI and PPy, and pure metal nanoparticles have been applied to improve the electrical conductivity of epoxy,[91] on the other hand, Al_2O_3,[92] boron nitride,[93–95] and graphitic materials such as graphene and CNTs can also provide epoxy with excellent thermal conductivity. The good thermal conductivity of materials can efficiently remove heat and address the heat dissipation problems of electronic devices.[96]

Graphene, a single atomic layer of graphitic carbon with a two-dimensional (2D) hexagonal structure,[97] has high thermal conductivity (4.84×10^3–5.30×10^3 W m^{-1} K^{-1}), high mechanical stiffness (130 GPa), a large specific surface area (2600 m^2 g^{-1}) and intrinsic carrier mobility (200 000 cm^2 V^{-1}).[98] These excellent physical properties allow graphene to serve as an efficient nanofiller to enhance the mechanical and conductive properties of epoxy.[99,100] For example, Bao *et al.*[46] synthesized hexachlorocyclotriphosphazene and glycidol modified graphene oxide (GO)/epoxy nanocomposites. The electrical conductivity of the functionalized graphene oxide/epoxy nanocomposites was improved by 6.5 orders of magnitude compared with that of the pure epoxy (10^{17} Ω cm). Tang *et al.*[101] introduced a polyetheramine functionalized reduced GO material to prepare GO/epoxy nanocomposites, which exhibited very good electrical conductivity (around 1.0×10^{-4} S cm^{-1} with the addition of 2.7 vol% functionalized GO), almost 11 orders of magnitude higher than that of the pure epoxy. Teng *et al.*[102] used pyrene molecules with a functional segmented poly(glycidyl methacrylate) polymer chain (Py–PGMA) to non-covalently functionalize graphene nanosheets (GNSs) through π–π stacking. After adding into epoxy, the thermal conductivity of these nanocomposites reached up to 1.91 W m^{-1} K^{-1}, which was about 20% and 267% higher than that of the pristine GNS/epoxy and the pristine MWNT/epoxy nanocomposites, respectively. Song *et al.*[103] introduced graphene flakes (GFs) with PBA into epoxy resins, the thermal conductivity of the GF/epoxy nanocomposites with a GF loading of 10 wt% achieved up to 1.53 W m^{-1} K^{-1}. Gu *et al.*[104] prepared graphite nanoplatelets with methanesulfonic acid/γ-glycidoxypropyltrimethoxysilane (f-GNPs) for the nanofiller of epoxy and the thermal conductivity was 1.698 W m^{-1} K^{-1} with a 30 wt% loading of f-GNPs, which was 8 times higher than that of the pure epoxy.

CNTs are derived from layers of graphene sheets and formed by rolling a piece of graphene to create a seamless cylinder, and have many unique physical properties including a light weight, large length-to-diameter ratio (132 000 000 : 1),[105] outstanding electrical and thermal conductivity as well as high tensile strength[106] with the Young's modulus of an individual CNT being higher than 1 TPa.[107,108] These properties make CNTs unique for preparing polymer nanocomposites. For example, Feng *et al.*[109] reported a mixed-curing-agent assisted layer-by-layer method to prepare CNT/epoxy nanocomposite films with a high CNT loading from 15 to 36 wt%. They obtained an electrical conductivity in the epoxy nanocomposites of up to 12 S cm^{-1}, which was much higher than that of the epoxy nanocomposites with low loadings of CNTs fabricated by a conventional method. Gu *et al.*[21] reported that the electrical conductivity of cured PANI functionalized MWNT/epoxy nanocomposites was improved by 5.5 orders of magnitude compared with the cured pure epoxy.

CNFs are composed of stacked truncated conical, or planar, graphene layers along the filament length.[110] CNFs have lower manufacturing costs than CNTs while maintaining a large aspect ratio, and high mechanical and electrical properties, which makes CNFs promising candidates for the development of novel polymer nanocomposites in large quantities. For example, Zhu *et al.*[2] prepared CNF/epoxy nanocomposites with a uniform nanofiller dispersion quality by introducing a functional amine terminated group (from silane) *via* silanization on the surface of the CNFs. Even though an enhanced tensile strength and strong interfacial interaction were obtained for the silanized CNF/epoxy nanocomposite, the electrical conductivity of the silane functionalized CNF/epoxy nanocomposite was decreased compared with that of the as-received CNF/epoxy nanocomposite at the same CNF loading, Fig. 12(a). The decreased electrical conductivity was due to the silane organo-layer on the surface of the CNFs, which partially hindered the effective electron transport pathway among the CNFs.

Conducting polymers including polyacetylene (PA), PANI, and PPy have gained more attention in the last few decades due to their remarkable conductivity[111] and wide applications in electronics,[112] electrodes for electrodeposition[113] and supercapacitors.[114] Normally, the conductivity of conducting polymers can be tuned through a doping process.[115] More recently, Zhang and Guo *et al.* have developed pure conducting polymers PANI[116] and PPy[17] as conducting nanofillers to improve the electrical conductivity of epoxy. The electrical conductivity of the epoxy was increased by 5–6 orders of magnitude after adding a 10.0 wt% loading of PANI nanofiller. The effect of different morphologies of the PANI nanofillers on the electrical conductivity of the epoxy was compared. The electrical conductivity of PANI nanofiber/epoxy nanocomposites was two orders of magnitude higher than that of the PANI nanosphere/epoxy nanocomposites associated with the contact resistance and percolation threshold.[116] Interestingly, PPy was used to serve as a coupling agent between Fe_3O_4 nanoparticles and an epoxy matrix.

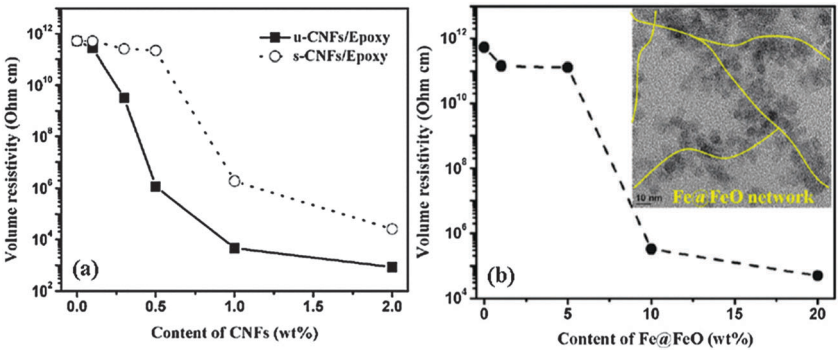

Fig. 12 Volume resistivity of (a) the cured pure epoxy and the cured epoxy nanocomposites filled with as-received CNFs (u-CNFs) and silane functionalized CNFs (s-CNFs);[2] (b) the cured pure epoxy and the cured epoxy filled with Fe@FeO nanoparticles. Inset shows the TEM image of Fe@FeO/epoxy nanocomposites, illustrating the conducting networks of Fe@FeO in the epoxy matrix.[32]

The electrical conductivity of the epoxy was improved by almost 7 orders of magnitude after adding 30 wt% of the PPy functionalized Fe_3O_4 nanoparticles.

Pure metallic nanoparticles have highly mobile electrons, which yield excellent electrical conductivity. However, owing to their easy oxidation and flammability in air, it is still challenging for them to be widely used in industry, most of the reported works focus on metal oxide nanoparticles.[85] For example, Zhu and Zhang *et al.* introduced a protecting shell including carbon[81] and metal oxide[32] thin layers to stabilize pure Fe nanoparticles. The volume resistivity of the prepared Fe@C/epoxy nanocomposites was improved by almost 7 orders of magnitude from 7.8×10^{13} (pure epoxy) to 1.2×10^{6} Ω cm (with a 20.0 wt% loading of Fe@C nanoparticles).[81] Meanwhile, the volume resistivity of the fabricated Fe@FeO/epoxy nanocomposites reached around 10^{5} Ω cm with a 20.0 wt% loading of Fe@FeO nanoparticles, Fig. 12(b).[32] The percolation threshold was observed in both the Fe@C and the Fe@FeO epoxy nanocomposites, at the 20.0 wt% nanoparticle loading level (the Fe@FeO nanoparticle loading was around 10.0 wt%), the nanoparticles constructed an infinite network structure for the electron transport among the nanoparticles within the epoxy matrix, leading to a huge change in the electrical conductivity of the epoxy nanocomposites.

In summary, among these conductive nanofillers, carbon species such as graphene, CNTs and CNFs could provide epoxy with the highest and the most efficient electrical conductivity (up to 11 orders of magnitude higher than that of pure epoxy). However, a proper functionalization method is required to prepare epoxy nanocomposites with better nanofiller dispersion quality since the surface modification may damage the structure of the carbon materials and destroy the electron transport pathway. Even the conducting polymers PANI and PPy were able to improve the electrical conductivity of epoxy by up to 7 orders of magnitude, but the presence of nitrogen atoms in the polymer backbone can provide a chemical reaction opportunity with the epoxy matrix as aforementioned, which may not be favorable for achieving high electrical conductivity in the conducting polymer/epoxy nanocomposites. The electrical conductivity of the metallic nanoparticle/epoxy nanocomposites could reach up to 7 orders of magnitudes higher than pure epoxy, which could be beneficial for the potential large quantity fabrication of electrically conductive epoxy nanocomposites.

In addition, epoxy is currently recognized as one of the most commonly used electrically conductive adhesives (ECAs) for microelectronic packaging such as flip-chip integrated circuit (IC) package assembly to a printed circuit board (PCB) due to its superior adhesive strength, good chemical and corrosion resistance, and low cost.[117] Normally, ECAs consist of an organic polymeric binder (such as epoxy) and conductive fillers. The epoxy serves as the mechanical bond for the interconnections, and the conductive fillers provide the electrical conductivity through the physical contact between the conductive fillers. The possible conductive fillers used include silver (Ag), gold (Au), nickel (Ni), copper (Cu) and various carbon materials (such as graphites and carbon nanotubes).[89,118,119] Silver flakes are the most commonly used and commercially available filler because of their high electrical conductivity and the nature of their conductive oxides. Even though nickel and copper are cost effective, they are easily oxidized at elevated temperatures and high humidity. These problems decrease the performance of the device interconnections.[120] Generally, ECAs can be categorized into isotropically conductive adhesives (ICAs, with 1–10 μm sized fillers), anisotropically conductive adhesives (ACAs, with typically 3–5 μm sized conductive fillers), and nonconductive adhesives (NCAs) depending on the conductive filler loading levels. Electrical conductivity for ICAs in all *x*-, *y*-, and *z*-directions can be achieved since the conductive filler loading level exceeds the percolation threshold. An example of the flip-chip bonding process using an ICA[120,121] is shown in Fig. 13. The conductive filler loading levels are far below the percolation threshold for ACAs and NCAs, which are not sufficient for inter-particle contact. Therefore, the electrical conductivity is exhibited only in the *z*-direction. ECAs have many advantages compared with conventional solder technology including environmental friendliness, mild processing conditions, low stress on substrates, and lightweight. However, many challenges still exist including low conductivity, and conductivity fatigue (decreased conductivity at elevated temperature and humidity aging) in reliability tests. These are the tasks for the researchers in this field to be solved in the future.

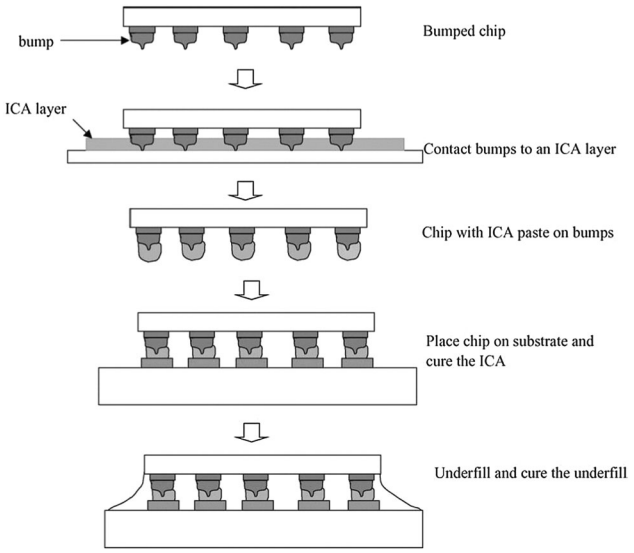

Fig. 13 A flip-chip bonding process using an ICA. Reprinted with permission from Elsevier.[121]

3.3 Epoxy nanocomposite flame retardancy

Although epoxy is one of the most important engineering polymers, the untreated epoxy is highly inflammable, which significantly limits its applications. Therefore, in order to improve its flame retardancy, the modification of epoxy is an imperative issue to be addressed.[122] Normally, reduced polymer flammability can be achieved through a combination of inherently flame retardant polymers such as polyimide, poly(*p*-phenylene-2,6-benzobisoxazole) (PBO), and poly(*p*-phenylene-2,6-benzobisthiazole) (PBZT), chemical modification of the existing polymers (for example, copolymerization of flame retardant monomers into the polymer chains), and incorporation of flame retardants into the hosting polymer matrix.[123] All of these methods can be applied to improve the flame retardancy of epoxy resins, such as a hyperbranched polyimide-modified epoxy system,[124] epoxy resin containing phosphorous (phosphorous from a synthesized silane coupling agent),[125] magnesium hydroxide ($Mg(OH)_2$)/epoxy,[126] functionalized layered double hydroxide (LDH)/epoxy,[127,128] antimony trioxide (Sb_2O_3)/epoxy,[129] aluminiumoxide trihydrate (ATH)/epoxy,[130] and 9,10-dihydro-9-oxa-10-phosphaphenanthrene-10-oxide (DOPO)/epoxy composites.[131] DOPO and its derivatives have been reported as novel phosphorous-containing flame retardants for epoxy resins.[132] Liao *et al.*[133] developed DOPO–reduced graphene oxide (DOPO–rGO) by grafting DOPO onto the surface of GO, which was then used as the nanofiller to fabricate epoxy nanocomposites. The DOPO–rGO/epoxy nanocomposites exhibited a significant increase in the char yield and limiting oxygen index (LOI) of about 81% and 30%, respectively, with the addition of 10 wt% DOPO–rGO. Yang *et al.*[134] synthesized tri(phosphaphenanthrene-maleimide-phenoxyl)-triazine (DOPO–TMT) as flame retardant additives for an epoxy matrix. The results demonstrated that the phosphorus- and nitrogen-free radicals released from the decomposition of DOPO–TMT preferred to form char residues with an intumescent and honeycombed structure, which endowed the epoxy with excellent flame retardant properties.

3.3.1 Phosphorus-, nitrogen- and silicon-based flame retardants. In the past decades, it was found that phosphorus-, nitrogen- and silicon-based flame retardants[123] could exhibit flame retardant performance in material compounds. Since they are friendly to the environment compared to halogenated compounds, these flame retardants are also called green products.[122,135] Normally, silicon can promote char formation in the condensed phase and trap the active radicals in the gas phase. The formed stable molecular compounds could stop decomposition arising from the introduced nitrogen and prevent the release of flammable gases. The presence of phosphorous could interrupt exothermic processes in the gas phase and promote char formation on the material surface in the condensed phase as a barrier.[123] Based on the aforementioned principles, Zhang *et al.* explored the flame retardancy performance of epoxy after mixing with different morphologies of PANI[116] and PPy[136] as the nanofillers (containing nitrogen). The heat release rate (HRR) results in Fig. 14 indicate that both PANI and PPy can reduce the HRR peak of the epoxy (with a 51.0% and 48.1% reduction of the HRR peaks for PANI and PPy, respectively) and the nanofiber morphology can decrease the HRR peak of the epoxy more than the nanosphere morphology due to the larger specific surface area. Gu *et al.*[18] introduced phosphoric acid doped PANI (containing phosphorous and nitrogen) into the silica/epoxy nanocomposites (containing silicon) and studied the flame retardant properties of these epoxy nanocomposites. The HRR peak of the epoxy nanocomposites filled with phosphoric acid

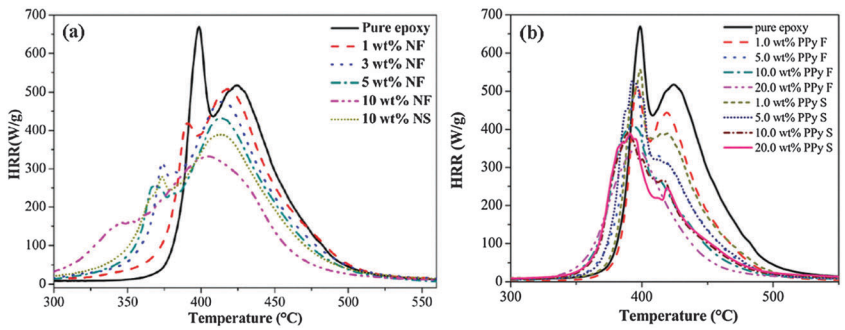

Fig. 14 (a) HRR *vs.* temperature curves of the cured pure epoxy and its nanocomposites with PANI nanofibers (NF) and nanospheres (NS);[116] (b) HRR *vs.* temperature curves of cured pure epoxy and its nanocomposites with PPy nanofibers (F) and nanospheres (S).[136]

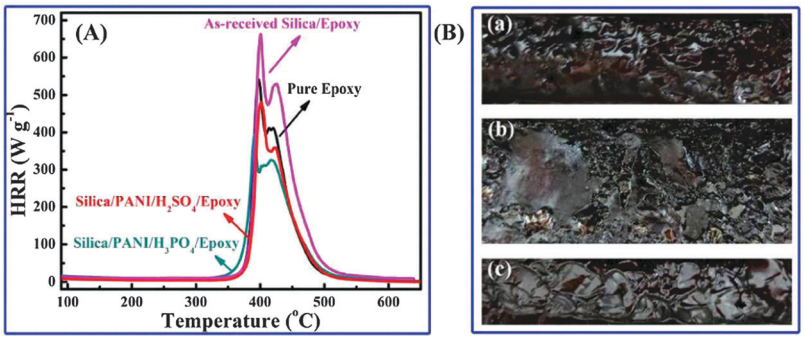

Fig. 15 (A) HRR *vs.* temperature of the pure epoxy and the epoxy nanocomposites filled with f-silica doped with H_3PO_4 and H_2SO_4; (B) photos of the (a) pure epoxy, and the silica/epoxy nanocomposites filled with 5.0 wt% (b) f-silica doped with H_3PO_4 and (c) f-silica doped with H_2SO_4 after combustion under nitrogen conditions from room temperature to 700 °C.[18]

doped PANI–silica (454.0 W g^{-1}) was much lower than that of the epoxy filled with sulfuric acid doped PANI–silica (478.8 W g^{-1}) and the as-received silica nanocomposites (533.8 W g^{-1}), Fig. 15(A). Meanwhile, the char residues of the epoxy nanocomposites filled with phosphoric acid doped PANI–silica were tightly cladded by the char yield, Fig. 15(B)b. However, the char residues of the epoxy filled with sulfuric acid doped PANI–silica were observed to migrate and be pushed to the surface by the volatile products (Fig. 15(B)c) and the char residues of the epoxy nanocomposites filled with the as-received silica exhibited a smooth and continual char layer due to the rapid volatilization (Fig. 15(B)a). These results further confirmed the role of the phosphorus component for the flame retardant performance of epoxy materials, showing that phosphorus can promote the char yield formation in the condensed phase.

Tang *et al.*[137] used glycidyl methacrylate (GMA) as a shell material to microencapsulate ammonium polyphosphate (MCAPP) by *in situ* polymerization (Fig. 16(a)) in order to link ammonium polyphosphate (APP) with an epoxy matrix and to provide the epoxy with the same flame retardant properties as the intumescent flame retardant. As shown in Fig. 16(b–d), after the cone calorimetry test, the residual char of the epoxy and MCAPP composite (Fig. 16(d)) exhibited dramatic *intumescentia* during the combustion process and formed a compact carbon layer compared with that of the pure epoxy (Fig. 16(b)) and the APP/epoxy composite (Fig. 16(c)). This indicated that MCAPP could promote the formation of intumescent carbonaceous char.

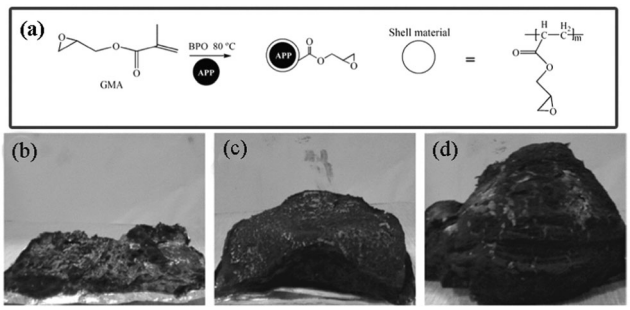

Fig. 16 (a) Reaction scheme for the formation of the MCAPP microcapsules; residue photos of samples at the end of a cone calorimetry test (b) pure epoxy, and epoxy nanocomposites (c) with an APP loading of 15 wt%, and (d) with a MCAPP loading of 15 wt%. Reprinted with permission from ACS publications.[137]

3.3.2 Graphene based flame retardants. Graphene is regarded as a favorable halogen-free flame retardant for epoxy due to its layered and graphitized structure, in which the graphene can behave as a physical barrier to adsorb the degraded products to facilitate the formation of char.[138] Normally, as-received graphene tends to decompose during combustion due to its weak thermal oxidation stability, which seriously reduces its flame retardant performance. Therefore, some modification to the as-received graphene is required to achieve an attractive flame retardant performance.[139] As an example, Qian *et al.*[140] reported a novel organic–inorganic hybrid flame retardant reduced graphene oxide material (FRs–rGO) by reacting reduced graphene oxide with (3-isocyanatopropyl)triethoxysilane and DOPO through an *in situ* sol–gel process, Fig. 17(A)a, to serve as the flame retardant additives to prepare epoxy nanocomposites, Fig. 17(A)b, which exhibited a significant improvement in the flame retardancy of the epoxy. Wang *et al.*[141] designed polyphosphamide covalently grafted graphene nanosheets (PPA-*g*-GNS) to serve as flame retardant additives to epoxy. Owing to the high phosphorous–nitrogen content, rich aromatic structure and graphitic structure, the PPA-*g*-GNS/epoxy composites demonstrated superior flame retardant properties. After being filled with 8 wt% PPA-*g*-GNS, the HRR peak of the epoxy composite was reduced by about 42% relative to that of the pure epoxy. Jiang *et al.*[142] fabricated Ce doped MnO_2–graphene hybrid sheets by utilizing electrostatic interactions between the Ce doped MnO_2 and the graphene sheets, and then mixed with an epoxy matrix. There are synergistic interactions between the Ce doped MnO_2 and graphene, in which the Ce doped MnO_2 served as a catalyst for the carbonization of degradation products and the graphene acted as a physical barrier to adsorb the degraded products to extend the contact time with the Ce doped MnO_2 catalyst. The Ce doped MnO_2–graphene/epoxy significantly suppressed the decomposition process of the epoxy during combustion. Wang *et al.*[143] synthesized a novel graphene-based hybrid (m-SGO) composed of graphene with nanosilica to alleviate the thermal-oxidation degradation of the graphitic structure, Fig. 17(B). After being filled into an epoxy matrix, an improved flame retardant performance was obtained because of the structure transformation.

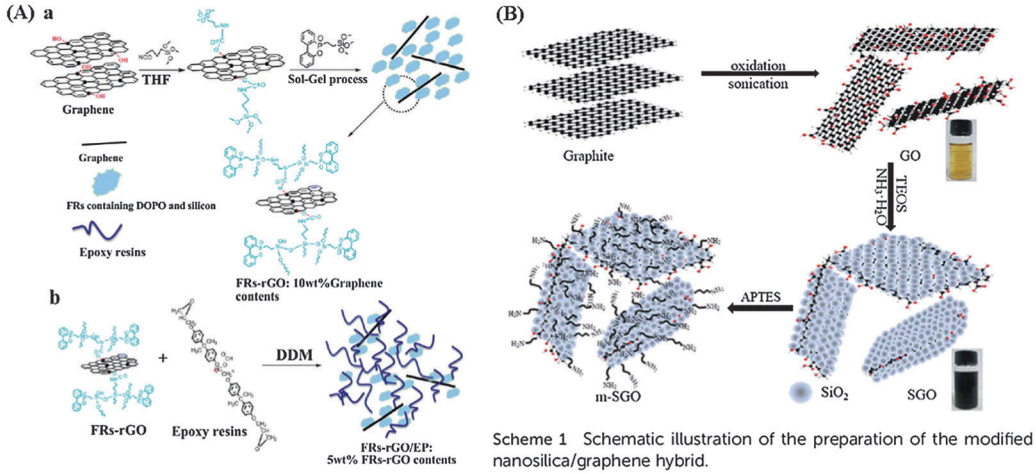

Scheme 1 Schematic illustration of the preparation of the modified nanosilica/graphene hybrid.

Fig. 17 Preparation procedure of (A) (a) FRs–rGO hybrids; (b) FRs–rGO/epoxy nanocomposites. Reprinted with permission from RSC Publishing;[140] (B) modified nanosilica/graphene hybrid. Reprinted with permission from RSC Publishing.[143]

Especially, the HRR peaks and total heat release of the modified epoxy filled with 1.5 wt% m-SGO were decreased by 39% and 10%, respectively, compared with those of the pure epoxy resin. The novel layered hybrid in the matrix was transformed into silica nanosheets and the obtained high resistance to oxidation degradation could delay the thermal degradation of the polymer chain segments during the combustion process. Yu *et al.*[144] prepared a functionalized reduced graphene oxide material (FRGO) wrapped with nitrogen and phosphorous, which was covalently incorporated into an epoxy matrix to form flame retardant epoxy nanocomposites, Fig. 18. The results demonstrated that the HRR peak of the FRGO/epoxy nanocomposites was diminished by about 43.0% with a FRGO loading of 2 wt% compared with that of the pure epoxy.

3.4 Other applications

3.4.1 Aeronautics and aerospace applications. Normally, the materials for aeronautic applications are subject to different environmental conditions including strong humidity, wide temperature variations, and many kinds of mechanical stresses such as compression, tension, torsion, and creep. Although the conventional materials such as aluminum, titanium, and steel can reach some of the requirements, they cannot achieve a compromise of low weight.[145] In the last few decades, innovative polymer composites in the aerospace industry have increased significantly as the load-carrying parts of new aircrafts such as the boeing 787, airbus 350, and F-35 for efficient weight reduction.[146] Epoxy based thermosetting nanocomposites are one of the most commonly used aeronautic materials in the aviation industry because

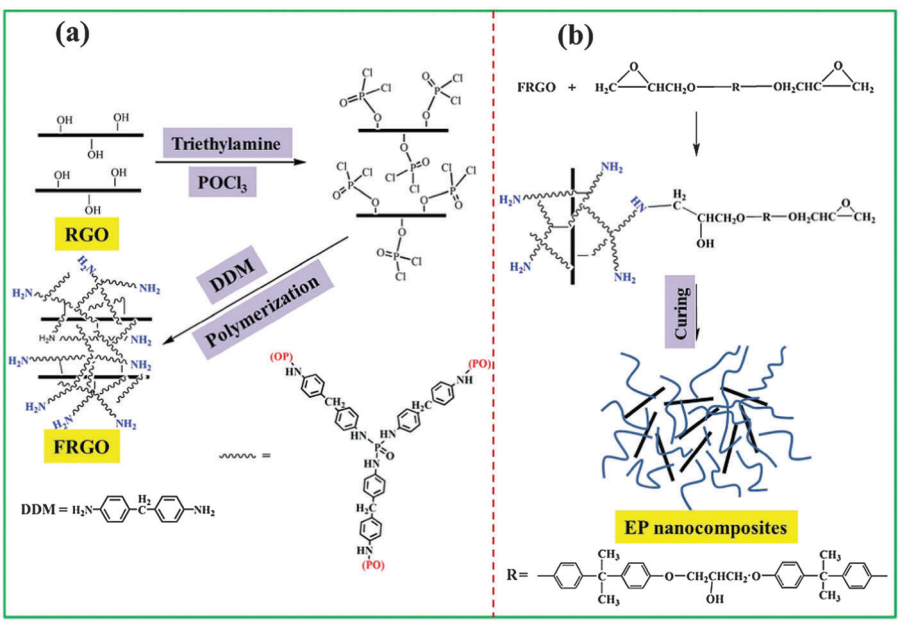

Fig. 18 Preparation procedure of (a) FRGO and (b) FRGO/epoxy nanocomposites. Reprinted with permission from RSC Publishing.[144]

of their excellent mechanical performance, chemical and electrical resistance and low shrinkage on curing.[15] In addition, multifunctionality has become an imperative aspect in aerospace technology in recent years. Multifunctional epoxy nanocomposites, which combine enhanced mechanical and thermal properties with sensing/actuating abilities, are in demand for the aerospace sector.[147] For example, in order to efficiently dissipate lightning currents without employing conductive metal fibers or metal screens, the electrical conductivity of structural parts such as aircraft fuselages has to reach 1–10 S m^{-1}.[145] Therefore, the exploitation of new advanced epoxy nanocomposites with additional functionalities without compromising structural integrity is required. In the past few years, novel CNT materials have served as excellent candidates to provide final products with enhanced structural integrity as well as multifunctionality. As aforementioned, CNTs have a high tensile strength with a high aspect ratio and excellent electrical conductivity, which make them a promising material for the actuation of a new generation of nano-reinforced composite systems in aerospace applications to replace the conventional materials. A more detailed review and analysis about CNT enhanced aerospace composites has been written by Paipetis and Kostopoulos.[147]

3.4.2 Automobile applications. Epoxy resin is one of the primary thermosetting resins used today in natural-fiber composites for automotive applications since epoxy resins can offer high performance and resistance to environmental degradation.[148] Typically, the epoxy based matrix composites used in the automotive industry serve as the power transmission drive shaft,[149] passenger car bumper beam,[150] door panels, seat backs, headliners, package trays, dashboards and interior parts,[151]and as an electrical conductive adhesive between a silicon chip and a lead frame of a package, and as a heat conductive adhesive between a silicon die and lead frame or substrate.[7] Normally, the usage of low-density natural fiber (such as kenaf, hemp, flax, jute, and sisal)–epoxy composites can reduce the car weight by about 10–30%. It's estimated that a 25% reduction of car weight is equal to saving 250 million barrels of crude oil annually.[150] Meanwhile, the natural fiber–epoxy composites exhibit low costs, low tool wearing rates, low production energy requirements, low health and safety risks, and good formability. They are less susceptible to the effects of stress concentration than metals.[152] Recently, in order to further improve the mechanical performance of natural fiber–epoxy composites, carbon nanofibers and glass fibers were introduced into natural fiber composites to form hybrid fiber reinforced epoxy composites, which can offer better fatigue characteristics since the micron cracks in the resin cannot propagate freely as in metals, but terminate at the strong hybrid fibers.[152] Therefore, parameters such as fiber orientation angles, stacking sequences, layer thickness and the number of layers should be altered in order to reach the required performance for automotive usage.[149]

3.4.3 Anti-corrosion coatings. Epoxy resins are not only used in aerospace and automotive applications, but also can be applied in marine systems, the retrofitting of structurally deficient bridges, the construction of new pedestrian and vehicular bridges as structural materials and as anti-corrosion coatings.[146] Nowadays, steel,[153] magnesium alloys,[154] aluminum,[11] and iron[45] are important parts of our daily life in automotive applications, household appliances, cellular phones, computers, guided weapons and heavy constructions such as marine and chemical industries. However, metal corrosion has become one increasingly severe problem in the metallic finishing industry.[155] It's estimated that corrosion-related maintenance costs between 70 and 120 billion dollars annually in the U.S.A. according to a NASA survey.[156] Therefore, many attempts and ingenious prevention methods to prevent corrosion have been invented.[157] Recently, epoxy coatings, as organic polymer coatings, have attracted considerable attention due to their excellent adhesion, high corrosion resistance, and environmental friendly properties.[158] Generally, epoxy coatings act as a physical barrier to prevent the aggression of deleterious species.[159] However, pristine epoxy cannot provide long-term anti-corrosive performance due to the presence of holes and defects over the coating surface after the curing process which are permeable to oxygen, water and corrosive ions such as Cl^- and H^+.[160] More recently, inorganic nanofillers such as SiO_2,[161] ZrO_2,[153] ZnO,[162] and nanoclay[163] have been introduced into epoxy matrices to form epoxy nanocomposites, and to modify the barrier effect of the epoxy for further boosting the anti-corrosive properties of the epoxy coating. It's reported that the nanoparticles could fill up the holes, micron cracks and defects of epoxy coatings, leading to improved anti-corrosive performance.[164] For example, Sari *et al.*[165] prepared polyester–amide hyperbranched polymer (HBP) modified nanoclay particles as a nanofiller to enhance the dispersion quality of nanoclay within an epoxy matrix and obtained an improved anti-corrosive performance of the epoxy coatings. The pure nanoclay was hydrophilic, which caused nanoparticle aggregation and poor intercalation in the epoxy coating, the bottom of Fig. 19. However, the HBP modified nanoclay showed a uniform distribution of the nanoparticles within the epoxy coating, the top of Fig. 19, which might effectively increase the length of the

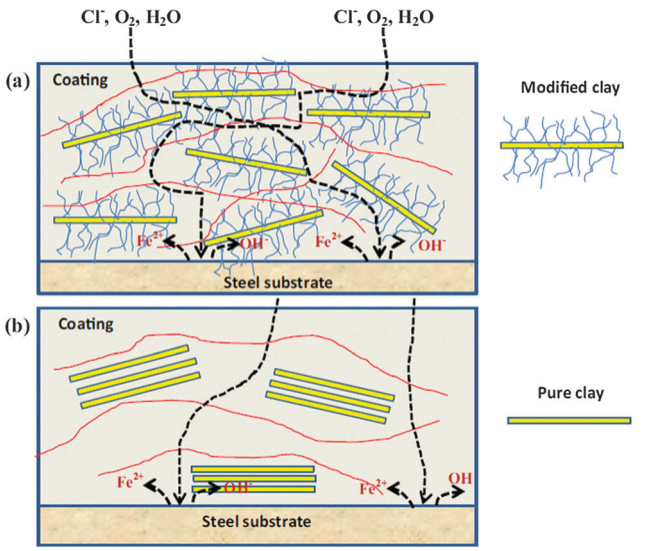

Fig. 19 Schematic illustration of (a) HBP modified nanoclay and (b) pure nanoclay in an epoxy coating. Reprinted with permission from Elsevier.[165]

diffusion pathways for corrosive electrolytes (such as Cl^-, O_2 and H_2O). To seek a new advanced modification method and a new type of nanofiller for epoxy nanocomposite coatings is a future task for researchers in the anti-corrosive field.

3.4.4 High voltage applications. Epoxy resin is one of the most widely used thermosets in high voltage (HV) apparatus including HV capacitors, printed circuit boards, generators, motors, and transformers as insulation because of its good mechanical and electrical properties, chemical stability and excellent processability.[166,167] Normally, the dielectric voltage breakdown strength (which is used to measure the failure strength of the insulation against the applied electric field) is the most important parameter in designing epoxy insulation materials.[168] Therefore, superior epoxy insulating materials require a higher thermal stability to avoid the occurrence of electrical breakdown.[169,170] As a consequence, the epoxy composites reinforced with micron sized inorganic fillers such as silica, alumina, *etc.* have emerged as the preferred insulating materials for HV applications due to their high dielectric breakdown voltage and improved thermal resistance compared with pure epoxy.[171] Recently, increased considerable interest has been dedicated to using nano-sized fillers as additives in epoxy matrices to form nanocomposites[172] since nanocomposite insulation can provide superior performances such as lower dielectric losses and increased dielectric strength, tracking and erosion resistance, and surface hydrophobicity compared with conventional micro-sized epoxy composites.[173] Singha *et al.*[174] observed that the dielectric permittivity in epoxy nanocomposites was lower than that in the pure epoxy and the epoxy with micro-sized filler at lower concentration (depending on the filler type and size) over a wide range of frequencies. Meanwhile, it has been found that the dielectric properties of insulation is also strongly related to the surface charge accumulation.[175] Nano-sized fillers at the surface of epoxy materials could result in corresponding changes in the electrical properties at the surface and suppress the surface charge accumulation, leading to decreased dielectric properties.[176,177]

4. Conclusion, challenges and perspective

This work has firstly discussed the challenges and solutions for the preparation of epoxy nanocomposites. The multifunctional epoxy nanocomposites with magnetic, electrically conductive, thermally conductive, and flame retardant properties of the past few years are reviewed in detail. The applications of epoxy nanocomposites in the aerospace, automotive, anti-corrosion coating, and high voltage fields are briefly summarized. In order to prepare epoxy nanocomposites with enhanced mechanical properties, the modification of nanofillers with functionalities to increase the dispersion quality of the nanofillers and to enhance the interfacial interaction between the nanofillers and the epoxy matrix is imperatively required. Epoxy nanocomposites with multifunctionalities still need to be developed to meet the demands for new applications of epoxy. Recently, Gu *et al.*[178] reported a strengthened magnetoresistive epoxy nanocomposite paper derived from synergistic Fe_3O_4–CNF nanohybrids, in which the epoxy nanocomposite paper was firstly observed to exhibit negative magnetoresistance of around −1.0% at a magnetic field of 9 T. This finding potentially broadens the application of epoxy to the flexible electronics, magnetoresistive sensors and printing industries. Therefore, to seek new functionalities of epoxy nanocomposites is the main task for researchers in the future.

Acknowledgements

This work is supported by the Shanghai Science and Technology Commission (14DZ2261100), the Science and Technology Commission of Shanghai Municipality (No. 15YF1412700), the Program for Young Excellent Talents in Tongji University (No. 2014KJ028), the National Natural Science Foundation of China (No. 51403175), the Shaanxi Natural Science Foundation of Shaanxi Province (No. 2015JM5153) and the Fundamental Research Funds for the Central Universities (No. 3102015ZY066). This work is also financially supported by the National Science Foundation (NSF)-Nanomanufacturing under the EAGER program (CMMI 13-14486), the Nanoscale Interdisciplinary Research Team and Materials Processing and Manufacturing (CMMI 10-30755) and Chemical and Biological Separations under the EAGER program (CBET 11-37441). The start-up funds from the University of Tennessee are also acknowledged.

References

1 K.-T. Hsiao, J. Alms and S. G. Advani, *Nanotechnology*, 2003, **14**, 791–793.
2 J. Zhu, S. Wei, J. Ryu, M. Budhathoki, G. Liang and Z. Guo, *J. Mater. Chem.*, 2010, **20**, 4937–4948.
3 X. Zhang, Q. He, H. Gu, H. A. Colorado, S. Wei and Z. Guo, *ACS Appl. Mater. Interfaces*, 2013, **5**, 898–910.
4 X. Zhang, O. Alloul, Q. He, J. Zhu, M. J. Verde, Y. Li, S. Wei and Z. Guo, *Polymer*, 2013, **54**, 3594–3604.
5 E. Tunce, I. Sauers, D. R. James, A. R. Ellis, M. P. Paranthaman, T. Aytuğ, S. Sathyamurthy, K. L. More, J. Li and A. Goyal, *Nanotechnology*, 2007, **18**, 025703.
6 V. A. Agubra and H. V. Mahesh, *J. Polym. Sci., Part B: Polym. Phys.*, 2014, **52**, 1024–1029.
7 P. Gromala, B. Muthuraman, B. Ozturk, K. Jansen and L. Ernst, Thermal, Mechanical and Multi-Physics Simulation and Experiments in Microelectronics and Microsystems (EuroSimE), 2015 16th International Conference, 2015.
8 H. Jin, C. L. Mangun, D. S. Stradley, J. S. Moore, N. R. Sottos and S. R. White, *Polymer*, 2012, **53**, 581–587.
9 X. Shi, T. A. Nguyen, Z. Suo, Y. Liu and R. Avci, *Surf. Coat. Technol.*, 2009, **204**, 237–245.
10 C. Acebo, X. Fernández-Francos, M. Messori, X. Ramis and À. Serra, *Polymer*, 2014, **55**, 5028–5035.
11 H. Abdollahi, A. Ershad-Langroudi, A. Salimi and A. Rahimi, *Ind. Eng. Chem. Res.*, 2014, **53**, 10858–10869.
12 B. Zhang, R. Asmatulu, S. A. Soltani, L. N. Le and S. S. A. Kumar, *J. Appl. Polym. Sci.*, 2014, **131**, 40286.

13 W. Tian, L. Liu, F. Meng, Y. Liu, Y. Li and F. Wang, *Corros. Sci.*, 2014, **86**, 81–92.
14 X.-L. Wang, Y.-Y. Yang, H.-J. Chen, Y. Wu and D.-S. Ma, *Tetrahedron*, 2014, **70**, 4571–4579.
15 A. Toldy, B. Szolnoki and G. Marosi, *Polym. Degrad. Stab.*, 2011, **96**, 371–376.
16 Y. Y. Liu, H. Wei, S. Wu and Z. Guo, *Chem. Eng. Technol.*, 2012, **35**, 713–719.
17 J. Guo, X. Zhang, H. Gu, Y. Wang, X. Yan, D. Ding, J. Long, S. Tadakamalla, Q. Wang, M. A. Khan, J. Liu, X. Zhang, B. L. Weeks, L. Sun, D. P. Young, S. Wei and Z. Guo, *RSC Adv.*, 2014, **4**, 36560–36572.
18 H. Gu, J. Guo, Q. He, S. Tadakamalla, X. Zhang, X. Yan, Y. Huang, H. A. Colorado, S. Wei and Z. Guo, *Ind. Eng. Chem. Res.*, 2013, **52**, 7718–7728.
19 M. Akatsuka, Y. Takezawa and S. Amagi, *Polymer*, 2001, **42**, 3003–3007.
20 P. Jyotishkumar, J. Koetz, B. Tiersch, V. Strehmel, C. Özdilek, P. Moldenaers, R. Hässler and S. Thomas, *J. Phys. Chem. B*, 2009, **113**, 5418–5430.
21 H. Gu, S. Tadakamalla, X. Zhang, Y. Huang, Y. Jiang, H. A. Colorado, Z. Luo, S. Wei and Z. Guo, *J. Mater. Chem. C*, 2013, **1**, 729–743.
22 S. V. Levchik and E. D. Weil, *Polym. Int.*, 2004, **53**, 1901–1929.
23 S. Sprenger, *J. Appl. Polym. Sci.*, 2013, **130**, 1421–1428.
24 E. P. Plueddemann, *J. Adhes. Sci. Technol.*, 1991, **5**, 261–277.
25 H. Lee and K. Neville, *Handbook of epoxy resins*, McGraw-Hill, New York, 1967.
26 A. A. Azeez, K. Y. Rhee, S. J. Park and D. Hui, *Composites, Part B*, 2013, **45**, 308–320.
27 H. Gu, J. Guo, H. Wei, X. Yan, D. Ding, X. Zhang, Q. He, S. Tadakamalla, X. Wang, T. C. Ho, S. Wei and Z. Guo, *J. Mater. Chem. C*, 2015, **3**, 8152–8165.
28 J. Guo, H. Gu, H. Wei, Q. Zhang, N. S. Haldolaarachchige, Y. Li, D. P. Young, S. Wei and Z. Guo, *J. Phys. Chem. C*, 2013, **117**, 10191–10202.
29 A. Paipetis and V. Kostopoulos, *Carbon nanotube enhanced aerospace composite materials: a new generation of multi-functional hybrid structural composites*, Springer Science & Business Media, 2012.
30 Y. Qing, X. Wang, Y. Zhou, Z. Huang, F. Luo and W. Zhou, *Compos. Sci. Technol.*, 2014, **102**, 161–168.
31 L.-J. Cui, H.-Z. Geng, W.-Y. Wang, L.-T. Chen and J. Gao, *Carbon*, 2013, **54**, 277–282.
32 J. Zhu, S. Wei, J. Ryu, L. Sun, Z. Luo and Z. Guo, *ACS Appl. Mater. Interfaces*, 2010, **2**, 2100–2107.
33 I. Zaman, T. T. Phan, H.-C. Kuan, Q. Meng, L. T. Bao La, L. Luong, O. Youssf and J. Ma, *Polymer*, 2011, **52**, 1603–1611.
34 M. A. Rafiee, J. Rafiee, Z. Wang, H. Song, Z.-Z. Yu and N. Koratkar, *ACS Nano*, 2009, **3**, 3884–3890.
35 J. H. Park and S. C. Jana, *Macromolecules*, 2003, **36**, 2758–2768.
36 K. Wang, L. Wang, J. Wu, L. Chen and C. He, *Langmuir*, 2005, **21**, 3613–3618.
37 J. Jang, J. Bae and K. Lee, *Polymer*, 2005, **46**, 3677–3684.
38 I. Park, H.-g. Peng, D. W. Gidley, S. Xue and T. J. Pinnavaia, *Chem. Mater.*, 2006, **18**, 650–656.
39 Y.-L. Liu, C.-Y. Hsu, W.-L. Wei and R.-J. Jeng, *Polymer*, 2003, **44**, 5159–5167.
40 Y.-Q. Li, S.-Y. Fu and Y.-W. Mai, *Polymer*, 2006, **47**, 2127–2132.
41 D. Sun, H.-J. Sue and N. Miyatake, *J. Phys. Chem. C*, 2008, **112**, 16002–16010.
42 Y. Liu, Z. Lin, W. Lin, K. S. Moon and C. P. Wong, *ACS Appl. Mater. Interfaces*, 2012, **4**, 3959–3964.
43 L. M. McGrath, R. S. Parnas, S. H. King, J. L. Schroeder, D. A. Fischer and J. L. Lenhart, *Polymer*, 2008, **49**, 999–1014.
44 A. Gonzalez-Campo, K. L. Orchard, N. Sato, M. S. P. Shaffer and C. K. Williams, *Chem. Commun.*, 2009, 4034–4036.
45 A. Olad, M. Barati and S. Behboudi, *Prog. Org. Coat.*, 2012, **74**, 221–227.
46 C. Bao, Y. Guo, L. Song, Y. Kan, X. Qian and Y. Hu, *J. Mater. Chem.*, 2011, **21**, 13290–13298.
47 J. Guo, J. Long, D. Ding, Q. Wang, Y. Shan, A. Umar, X. Zhang, B. L. Weeks, S. Wei and Z. Guo, *RSC Adv.*, 2016, **6**, 21187–21192.
48 D. Wang, R. Kou, D. Choi, Z. Yang, Z. Nie, J. Li, L. V. Saraf, D. Hu, J. Zhang, G. L. Graff, J. Liu, M. A. Pope and I. A. Aksay, *ACS Nano*, 2010, **4**, 1587–1595.
49 C.-M. Chan, J. Wu, J.-X. Li and Y.-K. Cheung, *Polymer*, 2002, **43**, 2981–2992.
50 Z. Guo, S. Wei, B. Shedd, R. Scaffaro, T. Pereira and H. T. Hahn, *J. Mater. Chem.*, 2007, **17**, 806–813.
51 Z. Wang, X. Yang, Q. Wang, H. T. Hahn, S.-g. Lee, K.-H. Lee and Z. Guo, *Int. J. Smart Nano Mater.*, 2011, **2**, 176–193.
52 Z. Guo, P. Tony, C. Oyoung, Y. Wang and H. T. Hahn, *J. Mater. Chem.*, 2006, **16**, 2800–2808.
53 Z. Guo, L. L. Henry, V. Palshin and E. J. Podlaha, *J. Mater. Chem.*, 2006, **16**, 1772–1777.
54 Z. Guo, L. L. Henry and E. J. Podlaha, *ECS Trans.*, 2006, **1**, 63–69.
55 J. R. Potts, D. R. Dreyer, C. W. Bielawski and R. S. Ruoff, *Polymer*, 2011, **52**, 5–25.
56 Z. Guo, K. Shin, A. B. Karki, D. P. Young and H. T. Hahn, *J. Nanopart. Res.*, 2009, **11**, 1441–1453.
57 P.-C. Ma, N. A. Siddiqui, G. Marom and J.-K. Kim, *Composites, Part A*, 2010, **41**, 1345–1367.
58 M. J. Green, N. Behabtu, M. Pasquali and W. W. Adams, *Polymer*, 2009, **50**, 4979–4997.
59 Q. He, T. Yuan, X. Yan, D. Ding, Q. Wang, Z. Luo, T. D. Shen, S. Wei, D. Cao and Z. Guo, *Macromol. Chem. Phys.*, 2014, **215**, 327–340.
60 J. Zhu, S. Wei, A. Yadav and Z. Guo, *Polymer*, 2010, **51**, 2643–2651.
61 Q. He, T. Yuan, X. Yan, Z. Luo, N. Haldolaarachchige, D. P. Young, S. Wei and Z. Guo, *Chem. Commun.*, 2014, **50**, 201–203.
62 C. A. Dyke and J. M. Tour, *Nano Lett.*, 2003, **3**, 1215–1218.
63 Y. Kang and T. A. Taton, *J. Am. Chem. Soc.*, 2003, **125**, 5650–5651.

64 Q. He, T. Yuan, S. Wei, N. Haldolaarachchige, Z. Luo, D. P. Young, A. Khasanov and Z. Guo, *Angew. Chem., Int. Ed.*, 2012, **51**, 8842–8845.
65 J. Zhu, S. Wei, Y. Li, L. Sun, N. Haldolaarachchige, D. P. Young, C. Southworth, A. Khasanov, Z. Luo and Z. Guo, *Macromolecules*, 2011, **44**, 4382–4391.
66 X. Zhang, Q. He, H. Gu, S. Wei and Z. Guo, *J. Mater. Chem. C*, 2013, **1**, 2886–2899.
67 Q. He, T. Yuan, X. Zhang, Z. Luo, N. Haldolaarachchige, L. Sun, D. P. Young, S. Wei and Z. Guo, *Macromolecules*, 2013, **46**, 2357–2368.
68 S. H. Park, S. H. Jin, G. H. Jun, S. Jeon and S. H. Hong, *Nano Res.*, 2011, **4**, 1129–1135.
69 D. Lee, S. H. Song, J. Hwang, S. H. Jin, K. H. Park, B. H. Kim, S. H. Hong and S. Jeon, *Small*, 2013, **9**, 2602–2610.
70 S. Zekri, *Synthesis and characterization of interfaces between naturally derived and synthetic nanostructures for biomedical applications*, ProQuest, 2007.
71 J. Gu, Q. Zhang, J. Dang, J. Zhang and S. Chen, *Polym. Bull.*, 2009, **62**, 689–697.
72 P. C. Ma, J.-K. Kim and B. Z. Tang, *Compos. Sci. Technol.*, 2007, **67**, 2965–2972.
73 H. Gu, S. Tadakamalla, Y. Huang, H. A. Colorado, Z. Luo, N. Haldolaarachchige, D. P. Young, S. Wei and Z. Guo, *ACS Appl. Mater. Interfaces*, 2012, **4**, 5613–5624.
74 D. Zhang, R. Chung, A. B. Karki, F. Li, D. Young and Z. Guo, *J. Phys. Chem. C*, 2010, **114**, 212–219.
75 Z. Guo, S. Park, H. T. Hahn, S. Wei, M. Moldovan, A. B. Karki and D. P. Young, *J. Appl. Phys.*, 2007, **101**, 09M511.
76 Z. Guo, S. E. Lee, H. Kim, S. Park, H. T. Hahn, A. B. Karki and D. P. Young, *Acta Mater.*, 2009, **57**, 267–277.
77 J. Zhu, S. Wei, N. Haldolaarachchige, D. P. Young and Z. Guo, *J. Phys. Chem. C*, 2011, **115**, 15304–15310.
78 R. Hao, R. Xing, Z. Xu, Y. Hou, S. Gao and S. Sun, *Adv. Mater.*, 2010, **22**, 2729–2742.
79 Y. Pan, X. Du, F. Zhao and B. Xu, *Chem. Soc. Rev.*, 2012, **41**, 2912–2942.
80 M. Colombo, S. Carregal-Romero, M. F. Casula, L. Gutiérrez, M. P. Morales, I. B. Böhm, J. T. Heverhagen, D. Prosperi and W. J. Parak, *Chem. Soc. Rev.*, 2012, **41**, 4306–4334.
81 X. Zhang, O. Alloul, J. Zhu, Q. He, Z. Luo, H. A. Colorado, N. Haldolaarachchige, D. P. Young, T. D. Shen, S. Wei and Z. Guo, *RSC Adv.*, 2013, **3**, 9453–9464.
82 H. Gu, Y. Huang, X. Zhang, Q. Wang, J. Zhu, L. Shao, N. Haldolaarachchige, D. P. Young, S. Wei and Z. Guo, *Polymer*, 2012, **53**, 801–809.
83 J. Park, K. Rhee and S. Park, *Appl. Surf. Sci.*, 2010, **256**, 6945–6950.
84 Y. Li, H. Zhu, H. Gu, H. Dai, Z. Fang, N. J. Weadock, Z. Guo and L. Hu, *J. Mater. Chem. A*, 2013, **1**, 15278–15283.
85 Z. Guo, K. Lei, Y. Li, H. W. Ng and H. T. Hahn, *Compos. Sci. Technol.*, 2008, **68**, 1513–1520.
86 X. Zhang, O. Alloul, Q. He, J. Zhu, M. J. Verde, Y. Li, S. Wei and Z. Guo, *Polymer*, 2013, **54**, 3594–3604.
87 J. W. Gu, Z. Y. Lv, Y. L. Wu, R. X. Zhao, L. D. Tian and Q. Y. Zhang, *Composites, Part A*, 2015, **79**, 8–13.
88 J. Gu, Z. Y. Lv, X. T. Yang, G. E. Wang and Q. Y. Zhang, *Sci. Adv. Mater.*, 2016, **8**, 972–979.
89 J. Gu, N. Li, L. D. Tian, Z. Y. Lv and Q. Y. Zhang, *RSC Adv.*, 2015, **5**, 36334–36339.
90 H. Wang and X. Wang, *ACS Appl. Mater. Interfaces*, 2013, **5**, 6255–6260.
91 Y. Chen, H.-B. Zhang, Y. Huang, Y. Jiang, W.-G. Zheng and Z.-Z. Yu, *Compos. Sci. Technol.*, 2015, **118**, 178–185.
92 J. Yu, X. Huang, L. Wang, P. Peng, C. Wu, X. Wu and P. Jiang, *Polym. Chem.*, 2011, **2**, 1380–1388.
93 X. Huang, C. Zhi, P. Jiang, D. Golberg, Y. Bando and T. Tanaka, *Adv. Funct. Mater.*, 2013, **23**, 1824–1831.
94 J. Gu, Q. Zhang, J. Dang and C. Xie, *Polym. Adv. Technol.*, 2012, **23**, 1025–1028.
95 J. Yu, X. Huang, C. Wu, X. Wu, G. Wang and P. Jiang, *Polymer*, 2012, **53**, 471–480.
96 J. Gu, J. J. Du, J. Dang, W. C. Geng, S. H. Hu and Q. Y. Zhang, *RSC Adv.*, 2014, **4**, 22101–22105.
97 H. Wang, H. Yi, C. Zhu, X. Wang and H. J. Fan, *Nano Energy*, 2015, **13**, 658–669.
98 H. Wang, H. Yi, X. Chen and X. Wang, *J. Mater. Chem. A*, 2014, **2**, 3223–3230.
99 M. Fang, Z. Zhang, J. Li, H. Zhang, H. Lu and Y. Yang, *J. Mater. Chem.*, 2010, **20**, 9635–9643.
100 M. Naebe, J. Wang, A. Amini, H. Khayyam, N. Hameed, L. H. Li, Y. Chen and B. Fox, *Sci. Rep.*, 2014, **4**, 4375.
101 G. Tang, Z.-G. Jiang, X. Li, H.-B. Zhang, S. Hong and Z.-Z. Yu, *Composites, Part B*, 2014, **67**, 564–570.
102 C.-C. Teng, C.-C. M. Ma, C.-H. Lu, S.-Y. Yang, S.-H. Lee, M.-C. Hsiao, M.-Y. Yen, K.-C. Chiou and T.-M. Lee, *Carbon*, 2011, **49**, 5107–5116.
103 S. H. Song, K. H. Park, B. H. Kim, Y. W. Choi, G. H. Jun, D. J. Lee, B. S. Kong, K. W. Paik and S. Jeon, *Adv. Mater.*, 2013, **25**, 732–737.
104 J. Gu, X. Yang, Z. Lv, N. Li, C. Liang and Q. Zhang, *Int. J. Heat Mass Transfer*, 2016, **92**, 15–22.
105 H. Gu, S. B. Rapole, Y. Huang, D. Cao, Z. Luo, S. Wei and Z. Guo, *J. Mater. Chem. A*, 2013, **1**, 2011–2021.
106 M.-F. Yu, B. S. Files, S. Arepalli and R. S. Ruoff, *Phys. Rev. Lett.*, 2000, **84**, 5552–5555.
107 H. Yi, H. Wang, Y. Jing, T. Peng and X. Wang, *J. Power Sources*, 2015, **285**, 281–290.
108 Y. Zhao and E. V. Barrera, *Adv. Funct. Mater.*, 2010, **20**, 3039–3044.
109 Q.-P. Feng, J.-P. Yang, S.-Y. Fu and Y.-W. Mai, *Carbon*, 2010, **48**, 2057–2062.
110 R. Vajtai, *Springer Handbook of Nanomaterials*, Springer, 2013.
111 H. Gu, J. Guo, X. Zhang, Q. He, Y. Huang, H. A. Colorado, N. S. Haldolaarachchige, H. L. Xin, D. P. Young, S. Wei and Z. Guo, *J. Phys. Chem. C*, 2013, **117**, 6426–6436.
112 H. Stoyanov, M. Kollosche, S. Risse, R. Waché and G. Kofod, *Adv. Mater.*, 2013, **25**, 578–583.
113 D. Wang, Q. Ye, B. Yu and F. Zhou, *J. Mater. Chem.*, 2010, **20**, 6910–6915.

114 H. Wei, J. Zhu, S. Wu, S. Wei and Z. Guo, *Polymer*, 2013, **54**, 1820–1831.
115 H. Gu, J. Guo, X. Yan, H. Wei, X. Zhang, J. Liu, Y. Huang, S. Wei and Z. Guo, *Polymer*, 2014, **55**, 4405–4419.
116 X. Zhang, Q. He, H. Gu, H. A. Colorado, S. Wei and Z. Guo, *ACS Appl. Mater. Interfaces*, 2012, **5**, 898–910.
117 I. D. Rosca and S. V. Hoa, *Compos. Sci. Technol.*, 2011, **71**, 95–100.
118 Y. Guan, X. Chen, F. Li and H. Gao, *Int. J. Adhes. Adhes.*, 2010, **30**, 80–88.
119 H. P. Wu, X. J. Wu, M. Y. Ge, G. Q. Zhang, Y. W. Wang and J. Jiang, *Compos. Sci. Technol.*, 2007, **67**, 1182–1186.
120 Y. Li, K.-S. J. Moon and C. Wong, *Nano-conductive adhesives for nano-electronics interconnection*, Springer, 2010.
121 Y. Li and C. P. Wong, *Mater. Sci. Eng., R*, 2006, **51**, 1–35.
122 P. M. Hergenrother, C. M. Thompson, J. G. Smith Jr, J. W. Connell, J. A. Hinkley, R. E. Lyon and R. Moulton, *Polymer*, 2005, **46**, 5012–5024.
123 S. Bourbigot and S. Duquesne, *J. Mater. Chem.*, 2007, **17**, 2283–2300.
124 F. L. Jin and S. J. Park, *J. Polym. Sci., Part B: Polym. Phys.*, 2006, **44**, 3348–3356.
125 C. H. Lin, C. C. Feng and T. Y. Hwang, *Eur. Polym. J.*, 2007, **43**, 725–742.
126 M. Zammarano, M. Franceschi, S. v. Bellayer, J. W. Gilman and S. Meriani, *Polymer*, 2005, **46**, 9314–9328.
127 E. N. Kalali, X. Wang and D.-Y. Wang, *J. Mater. Chem. A*, 2015, **3**, 6819–6826.
128 C. Li, J. Wan, E. N. Kalali, H. Fan and D.-Y. Wang, *J. Mater. Chem. A*, 2015, **3**, 3471–3479.
129 A. D. La Rosa, A. Recca, J. T. Carter and P. T. McGrail, *Polymer*, 1999, **40**, 4093–4098.
130 P. Kiliaris and C. D. Papaspyrides, *Prog. Polym. Sci.*, 2010, **35**, 902–958.
131 X. Wang, Y. Hu, L. Song, W. Xing, H. Lu, P. Lv and G. Jie, *Polymer*, 2010, **51**, 2435–2445.
132 P. Chao, Y. Li, X. Gu, D. Han, X. Jia, M. Wang, T. Zhou and T. Wang, *Polym. Chem.*, 2015, **6**, 2977–2985.
133 S.-H. Liao, P.-L. Liu, M.-C. Hsiao, C.-C. Teng, C.-A. Wang, M.-D. Ger and C.-L. Chiang, *Ind. Eng. Chem. Res.*, 2012, **51**, 4573–4581.
134 S. Yang, J. Wang, S. Huo, M. Wang and L. Cheng, *Ind. Eng. Chem. Res.*, 2015, **54**, 7777–7786.
135 Y. Shi, T. Kashiwagi, R. N. Walters, J. W. Gilman, R. E. Lyon and D. Y. Sogah, *Polymer*, 2009, **50**, 3478–3487.
136 X. Zhang, X. Yan, J. Guo, Z. Liu, D. Jiang, Q. He, H. Wei, H. Gu, H. A. Colorado, X. Zhang, S. Wei and Z. Guo, *J. Mater. Chem. C*, 2015, **3**, 162–176.
137 Q. Tang, B. Wang, Y. Shi, L. Song and Y. Hu, *Ind. Eng. Chem. Res.*, 2013, **52**, 5640–5647.
138 S. Liu, H. Yan, Z. Fang and H. Wang, *Compos. Sci. Technol.*, 2014, **90**, 40–47.
139 N. Hong, J. Zhan, X. Wang, A. A. Stec, T. R. Hull, H. Ge, W. Xing, L. Song and Y. Hu, *Composites, Part A*, 2014, **64**, 203–210.
140 X. Qian, L. Song, B. Yu, B. Wang, B. Yuan, Y. Shi, Y. Hu and R. K. Yuen, *J. Mater. Chem. A*, 2013, **1**, 6822–6830.
141 X. Wang, W. Xing, X. Feng, B. Yu, L. Song and Y. Hu, *Polym. Chem.*, 2014, **5**, 1145–1154.
142 S.-D. Jiang, Z.-M. Bai, G. Tang, L. Song, A. A. Stec, T. R. Hull, J. Zhan and Y. Hu, *J. Mater. Chem. A*, 2014, **2**, 17341–17351.
143 R. Wang, D. Zhuo, Z. Weng, L. Wu, X. Cheng, Y. Zhou, J. Wang and B. Xuan, *J. Mater. Chem. A*, 2015, **3**, 9826–9836.
144 B. Yu, Y. Shi, B. Yuan, S. Qiu, W. Xing, W. Hu, L. Song, S. Lo and Y. Hu, *J. Mater. Chem. A*, 2015, **3**, 8034–8044.
145 L. Guadagno, M. Raimondo, V. Vittoria, L. Vertuccio, C. Naddeo, S. Russo, B. De Vivo, P. Lamberti, G. Spinelli and V. Tucci, *RSC Adv.*, 2014, **4**, 15474–15488.
146 Y. Sugita, C. Winkelmann and V. La Saponara, *Compos. Sci. Technol.*, 2010, **70**, 829–839.
147 A. Paipetis and V. Kostopoulos, *Carbon nanotube enhanced aerospace composite materials: a new generation of multi-functional hybrid structural composites*, 2012.
148 E. Ghassemieh, *Materials in automotive application, state of the art and prospects*, INTECH Open Access Publisher, 2011.
149 M. Badie, E. Mahdi and A. Hamouda, *Mater. Des.*, 2011, **32**, 1485–1500.
150 M. Davoodi, S. Sapuan, D. Ahmad, A. Ali, A. Khalina and M. Jonoobi, *Mater. Des.*, 2010, **31**, 4927–4932.
151 J. Holbery and D. Houston, *JOM*, 2006, **58**, 80–86.
152 A. A. Talib, A. Ali, M. A. Badie, N. A. C. Lah and A. Golestaneh, *Mater. Des.*, 2010, **31**, 514–521.
153 M. Behzadnasab, S. Mirabedini, K. Kabiri and S. Jamali, *Corros. Sci.*, 2011, **53**, 89–98.
154 Y. Qiao, W. Li, G. Wang, X. Zhang and N. Cao, *RSC Adv.*, 2015, **5**, 47778–47787.
155 M. Hosseini, M. Jafari and R. Najjar, *Surf. Coat. Technol.*, 2011, **206**, 280–286.
156 C.-H. Chang, M.-H. Hsu, C.-J. Weng, W.-I. Hung, T.-L. Chuang, K.-C. Chang, C.-W. Peng, Y.-C. Yen and J.-M. Yeh, *J. Mater. Chem. A*, 2013, **1**, 13869–13877.
157 M. J. Hollamby, D. Fix, I. Dönch, D. Borisova, H. Möhwald and D. Shchukin, *Adv. Mater.*, 2011, **23**, 1361–1365.
158 A. M. Atta, A. M. El-Saeed, G. M. El-Mahdy and H. A. Al-Lohedan, *RSC Adv.*, 2015, **5**, 101923.
159 S. Pour-Ali, C. Dehghanian and A. Kosari, *Corros. Sci.*, 2014, **85**, 204–214.
160 M. Popović, B. Grgur and V. Mišković-Stanković, *Prog. Org. Coat.*, 2005, **52**, 359–365.
161 T.-C. Huang, Y.-A. Su, T.-C. Yeh, H.-Y. Huang, C.-P. Wu, K.-Y. Huang, Y.-C. Chou, J.-M. Yeh and Y. Wei, *Electrochim. Acta*, 2011, **56**, 6142–6149.
162 M. Rostami, S. Rasouli, B. Ramezanzadeh and A. Askari, *Corros. Sci.*, 2014, **88**, 387–399.
163 M. D. Tomić, B. Dunjić, V. Likić, J. Bajat, J. Rogan and J. Djonlagić, *Prog. Org. Coat.*, 2014, **77**, 518–527.
164 Z. Yu, H. Di, Y. Ma, L. Lv, Y. Pan, C. Zhang and Y. He, *Appl. Surf. Sci.*, 2015, **351**, 986–996.

165 M. G. Sari, B. Ramezanzadeh, M. Shahbazi and A. Pakdel, *Corros. Sci.*, 2015, **92**, 162–172.
166 R. Kochetov, T. Andritsch, P. Morshuis and J. Smit, 2010 Annual Report Conference on Electrical Insulation and Dielectric Phenomena (CEIDP), 2010.
167 Y. Xia, W. Wang, C. Tao, C. Li, S. He and W. Chen, Electrical Insulation Conference (EIC), 2015 IEEE, 2015.
168 A. Mohanty and V. Srivastava, *Mater. Des.*, 2013, **47**, 711–716.
169 S. Siddabattuni, T. P. Schuman and F. Dogan, *Mater. Sci. Eng., B*, 2011, **176**, 1422–1429.
170 Q. Wang and G. Chen, *Adv. Mater. Res.*, 2012, **1**, 93–107.
171 L. Meyer, E. Cherney and S. Jayaram, *IEEE Elect. Insul. Mag.*, 2004, **20**, 13–21.
172 C. Green and A. Vaughan, *IEEE Elect. Insul. Mag.*, 2008, **24**, 6–16.
173 G. Iyer, R. Gorur, R. Richert, A. Krivda and L. Schmidt, *IEEE Trans. Dielectr. Electr. Insul.*, 2011, **18**, 659–666.
174 S. Singha and M. J. Thomas, *IEEE Trans. Dielectr. Electr. Insul.*, 2008, **15**, 12–23.
175 B. Du, J. Zhang and Y. Gao, *IEEE Trans. Dielectr. Electr. Insul.*, 2012, **19**, 755–762.
176 A. Mohamad, G. Chen, Y. Zhang and Z. An, *IEEE Trans. Dielectr. Electr. Insul.*, 2015, **22**, 101–108.
177 Q. Wang, G. Chen and A. S. Alghamdi, Solid Dielectrics (ICSD), 2010 10th IEEE International Conference on, 2010.
178 H. Gu, J. Guo, H. Wei, S. Guo, J. Liu, Y. Huang, M. A. Khan, X. Wang, D. P. Young and S. Wei, *Adv. Mater.*, 2015, **27**, 6277–6282.

